1st International Student Research Conference -2020
Dhaka University Research Society (DURS), University of Dhaka, Bangladesh

Analyzing the Pattern of Land Use Land Cover Change and its Impact on Land Surface Temperature: A Remote Sensing Approach in Mymensingh, Bangladesh

Abdullah Al Rakib[1*], Kaniz Shaleha Akter[1], Md. Naimur Rahman[1], Sudipto Arpi[1], Abdulla - Al Kafy[1,2]

[1]Department of Urban & Regional Planning, Rajshahi University of Engineering & Technology, Rajshahi – 6203, Bangladesh
[2]Urban Planner & Project Officer (ICLEI South Asia), Rajshahi City Corporation, Rajshahi-6203, Bangladesh
**Corresponding Author Email: abdullahalrakib310@gmail.com*

Abstract:

Rapid urbanization creates a significant impact on urban land use land cover (LULC), increasing the land surface temperature (LST). Remote Sensing is one of the most proficient techniques for identifying the pattern of urban growth and LULC change in a particular region and its impact on urban LST variations. A significant increase in urban LST influenced by rapid LULC change substantially impacts the ecosystem, climate change, and accelerated global warming. Haphazard urban growth and lack of proper planning negatively impact natural resources (vegetation and water bodies) and result in a replacement with non-evaporating surfaces (urban area). This study used multi-temporal Landsat OLI/TM satellite data sets to analyze the impact of LULC changes on LST increase for two decades (1999, 2009, 2019) in Mymensingh city, Bangladesh. After becoming the divisional center, the result suggests that rapid urban growth takes place with a remarkable decrease in vegetation cover and water bodies in the study area. The urban growth almost doubled in the last 20 years, significantly increasing the LST by almost 8 °C. The LST distribution showed a higher concentration in urban areas, followed by bare land, vegetation cover, and water bodies. The study reveals that the decrease in urban green cover/wetlands and expansion in urban areas significantly increased the study area's surface temperature for the last two decades. This study will help urban planners, and environmental engineers quantify LULC change impacts on LST and proposed appropriate policy measures to control it.

Key Word*: Urban growth, land use land cover, land surface temperature, global warming, Landsat, Mymensingh.*

I. Introduction

Cities are the identity and initiator of modern urbanization process [1]. Development process enhances urbanization [2, 3]. This urban expansion can result changes in ecosystem, biodiversity, landscape and surrounding environment [2, 4, 5]. Though urbanization creates mass amount of development and prosperity in an area, it has certain demerits; both short and long-term [6, 7]. A long-term effect of this urbanization is the rapid increase in the land surface temperature (LST) [7, 8]. In these recent decades, rapid urban growth caused significant changes land use land cover (LULC) which had a negative impact on LST [9]. Currently, more than 50% of the people all over the world lives in urbanized areas [2, 10, 11]. This population is expected to increase to 6 billion by 2045 [11]. These urban inhabitants constantly take part in the economic progress and the regional exploitation of a city [12]. This development causes change in LULC which affects urban climate and the LST [13, 14]. Land cover (LC) usually means the part of the earth′s surface covered with natural resources and other natural features while land use (LU) means the area covered by humans for their personal uses but they are often considered studying together due to their strong interrelation [15]. LST can vary in both temporal and spatial features as a vast increase in LST can be seen in urban areas compared to the other LC [16]. In 1950, the urban area was only 3% which is expected to be increased to 66% by 2050 [17]. This rapid increase in the urban areas creates a major loss in the vegetation cover increasing the LST of that region, resulting creation of urban heat island (UHI) in these cities worldwide [18-20]. Dense vegetation is a cooling agent for the LST in the area [21]. In urban planning, LULC data are vital for long-term policy making [22]. And to detect changes in LULC, spatial mapping is one of the key tools to identify spatial and temporal change in an area [23].

For spatial mapping, satellite remote sensing (RS) in combination with Geographic Information System (GIS) is used all over world [12, 24]. Globally, Landsat data is used for this spatial mapping purpose as it has the longest continuous available record (nearly 45 years) [23]. GIS and RS is used globally to calculate ecosystem change and to observe global climate change in urban areas [6, 25-27]. Monitoring LULC changes and its impact on LST through direct field visits is time-consuming, error prone, and a matter of hard labor [28, 29]. On the other hand, RS and GIS technology is more efficient to evaluate, examine and map LULC and LST changes [30-33]. Several researchers have used GIS and RS data to analyze LULC change and its impact on LST with multi-temporal data [6, 8, 29, 34-40].

In Bangladesh, there are several studies related to LULC changes and its impact on LST change over the decades for various cities like Dhaka, Rajshahi, Chittagong, Cumilla, Khulna, etc. [34, 35, 40-43]. However, this type of analysis not that much available for Mymensingh City, the administrative headquarter of the new Mymensingh division of Bangladesh. Mymensingh City Corporation (MCC) area shows huge amount of urban growth, speacially in the last decade and many researcher believe it had a negative influence on the vast increase of temperature in that area. This study observes the LULC change in the MCC area for the past two decades (for the year 1999, 2009, 2019) and calculates the LST for those years using Multi-spectral Landsat data. This study also evaluates the relation of certain LC with the increase of LST and shows the increase in certain LC. Urban planners and policy makers will find this study useful for further planning of the urban growth in this city and to make it more environment friendly in the future.

II. Material And Methods

Study Area Profile

Mymensingh City is the divisional headquarter of the newly formed Mymensingh division [44]. In september 2011, the Mymensingh Zilla Nagorik Andolon resulted turning Mymensingh into the divisional capital and a city corporation. The city is located about 120 km north of Dhaka, the capital of Bangladesh.

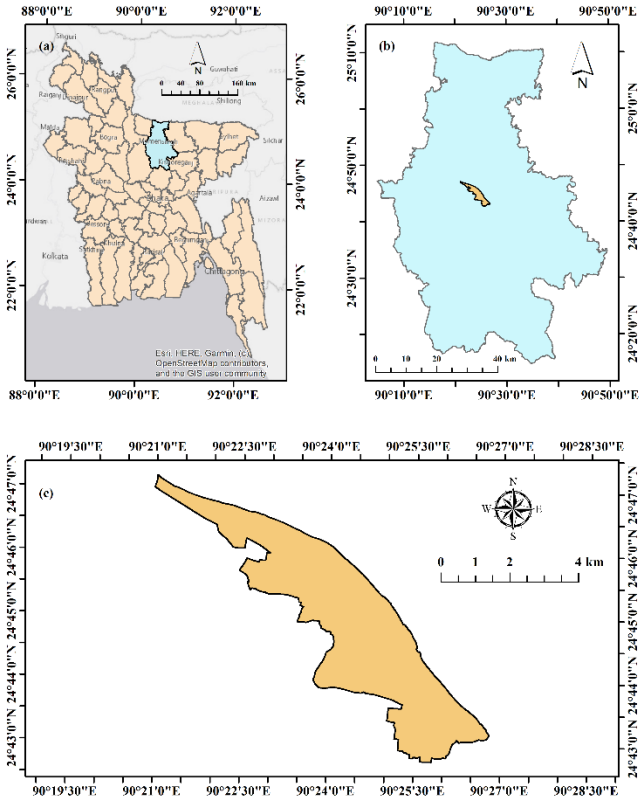

Figure no 1: Location map of the study area (a) Mymensingh district in Bangladesh (b) Mymensingh City corporation in the district (c) Mymensingh City Corporation area

Mymensingh city corporation has an area of 19.60 km^2 and Mymensingh municipality has a estimated population of 471,858 for 2018. Mymensingh is clearly observed from the old Brahmaputra river flowing along its north. The climate of this region is nearly same as Dhaka, having three major seasons, i.e. summer, monsoon and winter. The monsoon starts here from May or June and continue till August. In October to January, Mymensingh faces the winter season. The temperature rises in the end of January and the highest temperature can be recorded in February to mid-March. During this period, high sweating is caused by the increased level of humidity. Mymensingh city is well-known for the rapid urban growth after 1980s.

Data Acuqisition

Multi-spectral Landsat data was acquired from the USGS database to examine the LULC changes, LST variations, and the impact of LULC change on LST. Both summer and winter temperature were needed for this study. Thus, USGS data was downloaded for both of those seasons for the year 1999, 2009 and 2019. The study area lies into one scene of Landsat images, path 137 and row 043. The maximum cloud coverage was set to <10% during the satellite data downloading process but all the images contained almost zero cloud coverage over the study area. No additional process of geo-rectification or image to image registration process were done as Landsat data does not contain any kind of geometric and radiometric distortions [1]. The detailed information about the acquired data is shown in **Table 1**.

Table no 1: Detailed information of the acquired Landsat satellite data

Respective Year	Season	Date Acquired	Sensor	Path/Row	Multi-spectral band resolution	Thermal band resolution	Cloud Cover
1999	Summer	21 March 1999	TM	137/043	30 m	120 m (resampled to 30 m)	< 10%
	Winter	16 November 1999					
2009	Summer	28 February 2009					
	Winter	26 October 2009					
2019	Summer	24 February 2019	OLI			100 m (resampled to 30 m)	
	Winter	23 November 2019					

Source: US Geological Survey, 2020

Classification of LULC

For the study period, the data collected form the USGS database were divided into four LC classes. They were water bodies, urban areas, vegetation, and bare land using maximum likelihood classification (MLC) in ArcGIS 10.6 software. Band composition was performed for Landsat 5 TM and Landsat 8 OLI images where band 1 to 5 and band 7 were used for Landsat 5 images and band 1 to 7 were used for Landsat 8 images. Except water bodies, more than 100 signature files were taken for each LC classes. Due to the very low amount of water bodies, around 50 signature files were taken for this class.

For the accuracy calculation, more than 150 ground truth points (GCP) were acquired using Google Earth Engine (GEE) and global positioning system (GPS). Overall accuracy, user accuracy and Kappa Co-efficient were measured in the accuracy assessment. All the land cover images had overall accuracy of more than 84% and a Kappa Coefficient of more than 0.87.

LST estimation for Landsat 5 TM images

Both summer and winter season LST were measured for this study over the study period using Landsat Thermal bands. For Landsat 5 TM images, a three-step method was followed. The digital numbers (DN) of band 6 were converted to radiation luminance (R_{TM6}) using equation 1 – 3 [45, 46].

$$R_{TM6} = \frac{V}{255}(R_{max} - R_{min}) + R_{min} \dots\dots\dots (1)$$

Where V is the DN of band 6 and R_{max} = 1.896 (mW × cm^{-2} × sr^{-1}); R_{min} = 0.1534 (mW × cm^{-2} × sr^{-1}).
Then, the R_{TM6} is converted to Kelvin scale LST by using equation 2.

$$T_k = \frac{K_1}{\ln\left(\frac{K_2}{\frac{R_{TM6}}{b}}+1\right)} \dots\dots\dots (2)$$

where, K_1 (constant) = 1260.56 K and K_2 = 607.66 (mW × cm^{-2} × sr^{-1} μm^{-1}); b (spectral range) = 1.239 (μm).
Then, to convert the temperature into celcius scale, equation 3 is used.

$T_{^\circ C} = T_k - 273.15$ ... ... (3)

LST estimation for Landsat 8 OLI images

A seven-step method was followed to measure the LST for Landsat 8 OLI images.

Step 1: Band 10 and 11 is known as the thermal infrared sensor (TIRS) for Landsat 8 images. Band 2 – 5 were used separately to establish a spectral radiance (SR) data with equation 4 [47, 48].

$L = \left(\frac{L_{max} - L_{min}}{DN_{max}}\right) \times Band + L_{min}$ ... ... (4)

Here,
L = Atmospheric SR in watts/(m2 × srad × μm) ;Lmax = Maximum SR of respective Band; Lmin = Minimum SR of respective Band ; DNmax = Qcal max – Qcal min = maximum and minimum difference of sensor calibration.

Step 2: The metadata file has thermal constant value. After the conversion process of DNs to SR, the TIRS data has converted SR to BT. This process used equation 5 [49].

$$\mathrm{BT} = \frac{\mathrm{K_2}}{\ln\left(\frac{\mathrm{K_1}}{\mathrm{L_\lambda}} + 1\right)} - 273.15 \text{ ... ... (5)}$$

Step 3 and 4: The NDVI is calculated and its maximum and minimum value is used to calculate the proportion of vegetation (P_V) using equation 7 [50, 51].

$$\mathrm{NDVI} = \frac{\mathrm{NIR - R}}{\mathrm{NIR + R}} \text{ ... ... (6) [52, 53]}$$

$$\mathrm{P_V} = \left(\frac{\mathrm{NDVI - NDVI_{min}}}{\mathrm{NDVI_{max} - NDVI_{min}}}\right)^2 \text{ ... ... (7)}$$

Step 5: The land surface emissivity (LSE) is calculated after the previous process [50, 54].

$LSE = 0.004 \times P_V + 0.986$ ... ... (8)

Step 6: LST is evaluated for both band 10 and 11 using equation 9 [50, 51, 54].

$$LST = \frac{BT}{1 + \left(\frac{\lambda BT}{\rho}\right) \ln(LSE)} \text{ ... ... (9)}$$

where, λ is the wavelength of emitted radiance and ρ was calculated as: $\rho = h\ c\ \sigma = 1.438 \times 10\text{-}2$ mk.
Here, $\sigma = 1.38 \times 10{-}23$ J/K, h (Planck's constant) = $6.626 \times 10{-}34$ J s, and c (velocity of light) = 2.998×108 m/s [48, 50].

Step 7: To calculate the acutal LST, using cell statistics tool in ArcGIS 10.6 software, an average of both LST of band 10 and 11 is evaluated for the study area.

LST variation over different LULC

The LST value does not remain the same over all the LC in one area. It fluctuates between low value in vegetation covers and water bodies to higher values in impervious surfaces of urban areas or bare lands. To calculate this variation for the four LC classes of the study area over the study period, tabulate area tool was used in ArcGIS 10.6 for both summer and winter season.

III. Result and Discussion

LULC Change Analysis

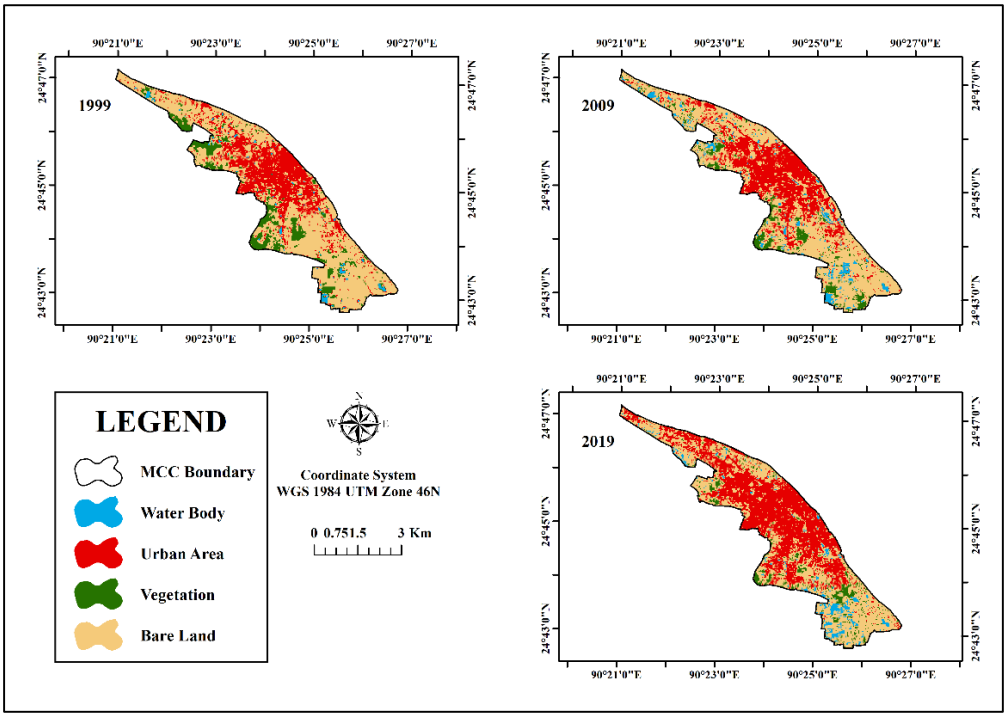

Figure no 2: LULC Map of the study area for the year 1999, 2009 and 2019

The MLC algorithm was used for the classification process over the study period for MCC area (**Figure 2**). Two trends of land cover change clearly stood out. The vast increase in urban areas and the gradual decrease in the vegetation areas and bare lands. In 1999, very low amount of water bodies (1.79%) and vegetation area (7.73%) was there. The maximum LC in the study area was in bare land (59.35%) (**Table 2**). From 1999 – 2009, urban areas increased by 9.91% and the vegetation area decreased by 34.48%. Remarkable increase in urban areas was also seen in 2009 – 2019 period, where it increased by 48.85%. During this period, significant decrease in other LC is also seen. Water bodies decreased by 13.23%, vegetation cover decreased by 27.65% and bare land decreased by 20.36%. During the whole study period, an increase of 63.60% of urban areas was seen in the study areas whereas 52.59% decrease in vegetation land and 22.44% decrease in the bare land was also recorded. This gradual decrease is caused by the replacement of bare land and water bodies with urban areas. Haphazard and unplanned growth in the study area caused this scenario of gradual decrease of bare land and vegetation cover.

Table No 2: Area change in different land cover

LULC Type	Area (in sqkm)			Area (in %)			Change (in %)		
	1999	2009	2019	1999	2009	2019	1999 - 2009	2009 - 2019	1999 - 2019
Water Body	0.35	0.93	0.80	1.79	4.72	4.10	163.59	-13.23	128.72
Urban Area	5.30	5.83	8.68	27.07	29.75	44.28	9.91	48.85	63.60
Vegetation	2.31	1.51	1.10	11.79	7.73	5.59	-34.48	-27.65	-52.59
Bare Land	11.63	11.33	9.02	59.35	57.81	46.03	-2.61	-20.36	-22.44

LST scenario for the study period

Spatial-temporal distribution in the study area for both summer and winter season was calculated, discussed in **section II.** The yearly distribution for summer and winter season is shown in **Figure 3 and 4**. The increasing scenario for both seasons is clearly visible and the detailed observation is shown in **Table 3**. In 1999, the highest temperature was

26.57˚C and 21.42˚C which increased to 29.43˚C and 25.25˚C in 2009 for summer and winter season respectively. The maximum area (46.16%) in 1999 for summer season fall in 24˚C - <28˚C. As for the winter scenario, maximum area fall in <20 ˚C range. For 2009 scenario, maximum area for summer season (44.44%) fall in 28 ˚C - <32 ˚C and for winter season (42.59%) 24 ˚C - <28 ˚C range had the highest percentage of area. In 2019, the scenario changed for both seasons.

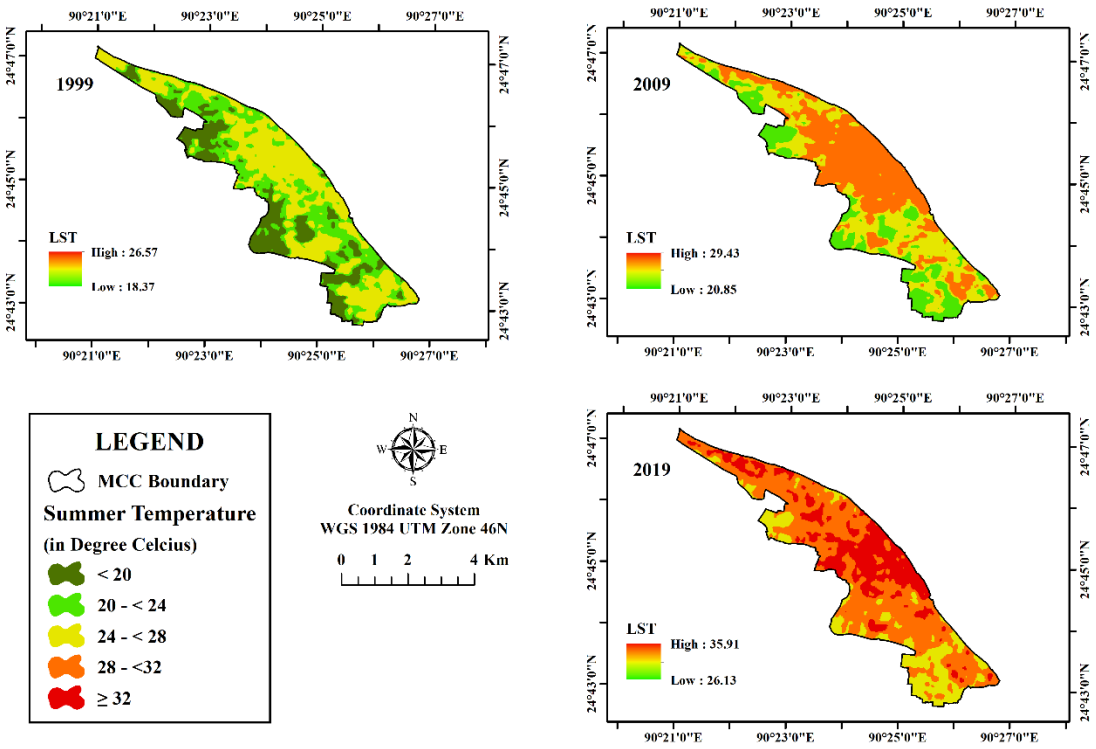

Figure no 3: LST distribution for summer season of 1999, 2009 and 2019

In 2019, the maximum temperature was 35.91˚C and 29.74˚C for summer and winter season respectively. For summer season, no area fall in <20 ˚C and 20 ˚C - <24 ˚C range, where for winter season the temperature range started from 20 ˚C - <24 ˚C. 28 ˚C - <32 ˚C range covered most of the areas (55.61%) for 2019 summer scenario whereas 24 ˚C - <28 ˚C had the most area (51.58%) covered during the winter scenario for the same year.

Table No 3: Seasonal LST scenario for both summer and winter season over the study period

Temperature Range (in degree celcius)	Area (in sqkm)						Area (in %)					
	Summer			Winter			Summer			Winter		
	1999	2009	2019	1999	2009	2019	1999	2009	2019	1999	2009	2019
< 20	4.61	0.00	0.00	11.98	6.58	0.00	23.52	0.00	0.00	61.16	33.59	0.00
20-<24	5.94	4.00	0.00	7.61	4.67	2.52	30.32	20.41	0.00	38.84	23.82	12.86
24-<28	9.05	6.89	3.71	0.00	8.35	10.11	46.16	35.15	18.95	0.00	42.59	51.58
28-<32	0.00	8.71	10.90	0.00	0.00	6.97	0.00	44.44	55.61	0.00	0.00	35.56
≥ 32	0.00	0.00	4.98	0.00	0.00	0.00	0.00	0.00	25.44	0.00	0.00	0.00

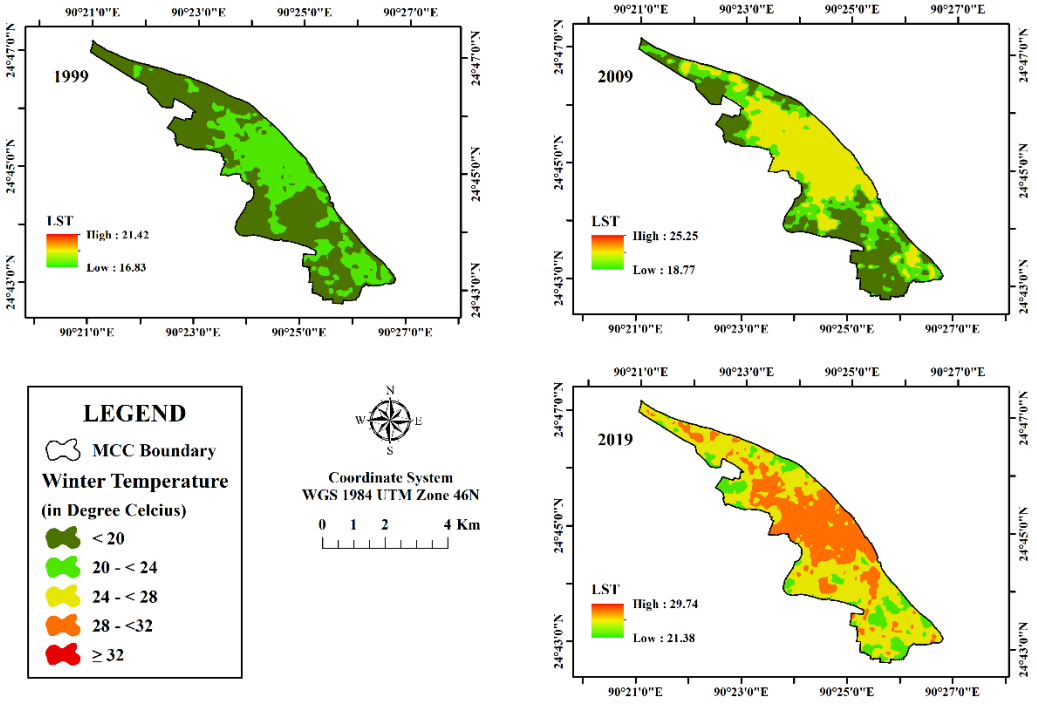

Figure no 4: LST distribution for winter season for 1999, 2009 and 2019.

Reduction of vegetaion covers, climate change, hapharazard urban growth, and unplanned urbanization is the primary reasons behind this rapid increase of LST [55-57]. The climate change experts and the metrologists suggest that the winter season in the upcoming years will be shorter than the previous years due to low falling amount of mercury [58]. Unchecked growth in LST will soon result bad affect on ecosystem eliminating rare plants, species and other natural features, lowering groundwater level, and will create shortage in livestock [59].

LST distribution in different LC (Summer Season)

Spatial distribution of LST in different LC shows higher concentration of high temperature in urban areas and bare lands. As vegetation LC is considered as a cooling agent in LST, low temperature scenario is seen in vegetation covers. Maximum temperature for summer season in 1999 fall in 24˚C - <28 ˚C range having 18.05% area in urban areas and 27.69% of area in bare lands. In 2009, urban area had the maximum concentration (25.05%) in the highest temperature range, i.e., 28 ˚C - <32 ˚C with 18.66% of the area in bare lands. In 2019, the maximum range was ≥32 ˚C which had the most concentration of area (20.51%) in urban land cover. Also, for the 28 ˚C - <32 ˚C, urban areas (23.46%) and bare lands (28.42%) had the most percentage of areas.

Table no 4: LST(Summer) distribution in over different LC

LULC	LST Range in ˚C									
	< 20		20 - < 24		24 - < 28		28 - < 32		≥ 32	
	Area (sqkm)	Area (%)	Area (sqkm)	Area (%)	Area (sqkm)	Area (%)	Area (sqkm)	Area (%)	Area (sqkm)	Area (%)
1999 Summer Season										
Water Body	0.23	1.19	0.08	0.41	0.04	0.19	0.00	0.00	0.00	0.00
Urban Area	0.29	1.47	1.48	7.55	3.54	18.05	0.00	0.00	0.00	0.00
Vegetation	2.01	10.27	0.25	1.29	0.05	0.23	0.00	0.00	0.00	0.00
Bare Land	2.07	10.59	4.13	21.08	5.43	27.69	0.00	0.00	0.00	0.00
2009 Summer Season										
Water Body	0.00	0.00	0.58	2.94	0.26	1.31	0.09	0.47	0.00	0.00

Urban Area	0.00	0.00	0.05	0.25	0.87	4.45	4.91	25.05	0.00	0.00
Vegetation	0.00	0.00	1.11	5.67	0.35	1.80	0.05	0.26	0.00	0.00
Bare Land	0.00	0.00	2.26	11.55	5.41	27.60	3.66	18.66	0.00	0.00
2019 Summer Season										
Water Body	0.00	0.00	0.00	0.00	0.55	2.81	0.24	1.24	0.01	0.05
Urban Area	0.00	0.00	0.00	0.00	0.06	0.31	4.60	23.46	4.02	20.51
Vegetation	0.00	0.00	0.00	0.00	0.61	3.09	0.49	2.49	0.00	0.01
Bare Land	0.00	0.00	0.00	0.00	2.50	12.75	5.57	28.42	0.95	4.87

LST distribution in different LC (Winter Season)

Winter scenario also shows higher concentration of urban areas in higher temperature areas. For 1999, only two ranges were present in the study areas. The higest temperature fall in 20˚C - <24 ˚C range, having 19.50% of urban areas nad 18.50% of bare lands. As vegetation area is a cooling agent, 11.16% of vegetation cover fall in <20 ˚C in the same year. In 2009, the highest temperature fall in 24 ˚C - <28 ˚C range, where 25.79% of urban area was present and 15.85% of bare land was present. In 2019 scenario, higher temperature fall in 28 ˚C - <32 ˚C range, where 29.06% of urban areas were present with 15.04% of urban areas falling in 24 ˚C - <28 ˚C range. The highest amount of bare land were present in 24 ˚C - <28 ˚C, having 31.13% of bare land.

Table no 5: LST(Winter) distribution in different LC

LULC	LST Range in ˚C									
	< 20		20 - < 24		24 - < 28		28 - < 32		≥ 32	
	Area (sqkm)	Area (%)	Area (sqkm)	Area (%)	Area (sqkm)	Area (%)	Area (sqkm)	Area (%)	Area (sqkm)	Area (%)
1999 Winter Season										
Water Body	0.31	1.58	0.04	0.21	0.00	0.00	0.00	0.00	0.00	0.00
Urban Area	1.48	7.56	3.82	19.50	0.00	0.00	0.00	0.00	0.00	0.00
Vegetation	2.19	11.16	0.12	0.63	0.00	0.00	0.00	0.00	0.00	0.00
Bare Land	8.01	40.85	3.63	18.50	0.00	0.00	0.00	0.00	0.00	0.00
2009 Winter Season										
Water Body	0.64	3.28	0.19	0.96	0.09	0.48	0.00	0.00	0.00	0.00
Urban Area	0.12	0.62	0.65	3.34	5.05	25.79	0.00	0.00	0.00	0.00
Vegetation	1.11	5.67	0.31	1.59	0.09	0.46	0.00	0.00	0.00	0.00
Bare Land	4.71	24.02	3.51	17.94	3.11	15.85	0.00	0.00	0.00	0.00
2019 Winter Season										
Water Body	0.00	0.00	0.36	1.82	0.41	2.10	0.03	0.17	0.00	0.00
Urban Area	0.00	0.00	0.04	0.18	2.95	15.04	5.69	29.06	0.00	0.00
Vegetation	0.00	0.00	0.43	2.17	0.65	3.31	0.02	0.11	0.00	0.00
Bare Land	0.00	0.00	1.70	8.68	6.10	31.13	1.22	6.22	0.00	0.00

IV. Conclusion

This study was conducted to find out the changes in LULC in the MCC area and its impact on LST with detailed observation of spatial distribution of LST over different LC. This study reveals that over the last two decades, urban areas increased by 63.60%. This rapid expansion of this urban areas resulted in 52.59% and 22.44% decrease in vegetation and bare land respectively for 1999 – 2019. This unplanned change in LULC resulted rapid increase in LST for both summer and winter season over the study period. The LST changing trend shows that the maximum temperature during the summer and winter season increased by 8 ˚C in summer seasons and 5 ˚C in winter season over the last two decades, having most of the higher temperature areas in urban areas and bare lands.

To control this urban growth and the rapid increase of this temperature resulted great harm in the ecosystem and lowered the ground water level, with creating unbearable loss in the greener areas. A planned approach in the development of policies and urban expansion will result placement of different urban features in proper places. This planned approach will preserve the vegetation cover and will result in a more controlled temperature scenario in the study area. Urbanization is not a phenomena that can be stopped entirely, but it can be controlled with proper planning and policies which will ensure adequate housing for all the people with a balanced ecosystem and nature. This study will help the urban planners and policy makers to understand the current situation in Mymensingh city and to make a decision which will make this city more sustainable and eco-friendly.

References

[1] A. A. Kafy, M. S. Rahman, A. A. Faisal, M. M. Hasan, and M. Islam, "Modelling future land use land cover changes and their impacts on land surface temperatures in Rajshahi, Bangladesh," *Remote Sensing Applications: Society and Environment,* 2020.

[2] U. Habitat, "Urbanization and development: emerging futures," vol. 3, no. 4, pp. 4-51, 2016.

[3] M. S. Rahman, H. Mohiuddin, A.-A. Kafy, P. K. Sheel, and L. Di, "Classification of cities in Bangladesh based on remote sensing derived spatial characteristics," *Journal of Urban Management,* 2018.

[4] H. Bahi, H. Rhinane, A. Bensalmia, U. Fehrenbach, and D. Scherer, "Effects of urbanization and seasonal cycle on the surface urban heat island patterns in the coastal growing cities: A case study of Casablanca, Morocco," *Remote Sensing,* vol. 8, no. 10, p. 829, 2016.

[5] M. L. McKinney, "Urbanization, biodiversity, and conservation. Bioscience 52: 883890McKinney ML (2006) Urbanization as a major cause of biotic homogenization," *Biol Conserv,* vol. 127, p. 247260, 2002.

[6] B. Celik, S. Kaya, U. Alganci, and D. Z. Seker, "Assessment of the Relationship Between Land Use/Cover Changes and Land Surface Temperatures: A case study of Thermal Remote Sensing," *FEB-FRESENIUS ENVIRONMENTAL BULLETIN,* vol. 3, p. 541, 2019.

[7] M. Maimaitiyiming *et al.*, "Effects of green space spatial pattern on land surface temperature: Implications for sustainable urban planning and climate change adaptation," *Journal of Photogrammetry and Remote Sensing,* vol. 89, pp. 59-66, 2014.

[8] J. Mallick, Y. Kant, and B. Bharath, "Estimation of land surface temperature over Delhi using Landsat-7 ETM+," *J. Ind. Geophys. Union,* vol. 12, no. 3, pp. 131-140, 2008.

[9] B. Yuen and L. Kong, "Climate change and urban planning in Southeast Asia," *Surveys Perspectives Integrating Environment Society,* no. 2.3, 2009.

[10] T. G. McGee, *The urbanization process in the third world*. London: G. Bell and Sons, Ltd, 1971.

[11] A. A. Kafy, M. Rahman, A. Rakib, S. Arpi, and A.-A. Faisal, "Assessing Satisfaction Level of Urban Residential Area: A Comparative Study Based on Resident's Perception in Rajshahi City, Bangladesh," in *1st International Conference on Urban and Regional Planning, Bangladesh*, Dhaka , Bangladesh, 2019, pp. 225 - 235: Bangladesh Institute of Planners

[12] Q. Weng, "A remote sensing-GIS evaluation of urban expansion and its impact on surface temperature in the Zhujiang Delta, China," *International Journal of Remote Sensing,* vol. 22, 2001// 2001.

[13] M. Herold, N. C. Goldstein, and K. J. Clarke, "The spatiotemporal form of urban growth: measurement, analysis and modeling," *Remote sensing of Environment,* vol. 86, no. 3, pp. 286-302, 2003.

[14] J. Xiao *et al.*, "Evaluating urban expansion and land use change in Shijiazhuang, China, by using GIS and remote sensing," *Landscape and Urban Planning,* vol. 75, no. 1-2, pp. 69-80, 2006.

[15] P. H. Verburg, J. Van De Steeg, A. Veldkamp, and L. Willemen, "From land cover change to land function dynamics: a major challenge to improve land characterization," *Journal of Environmental Management,* vol. 90, no. 3, pp. 1327-1335, 2009.

[16] Y. Zhang, H. Balzter, B. Liu, and Y. Chen, "Analyzing the impacts of urbanization and seasonal variation on land surface temperature based on subpixel fractional covers using Landsat images," *IEEE Journal of Selected Topics in Applied Earth Observations and Remote Sensing,* vol. 10, no. 4, pp. 1344-1356, 2016.

[17] (2018). *World Urbanization Prospects: The 2018 Revision, Online Edition*.

[18] C. Yang *et al.*, "Mapping the influence of land use/land cover changes on the urban heat island effect—A case study of Changchun, China," *Sustainability,* vol. 9, no. 2, p. 312, 2017.

[19] Ahmed, "Assessment of urban heat islands and impact of climate change on socioeconomic over Suez Governorate using remote sensing and GIS techniques," *The Egyptian Journal of Remote Sensing and Space Science,* vol. 21, no. 1, pp. 15-25, 2018.

[20] M. El-Hattab, S. Amany, and G. Lamia, "Monitoring and assessment of urban heat islands over the Southern region of Cairo Governorate, Egypt," *The Egyptian Journal of Remote Sensing Space Science,* vol. 21, no. 3, pp. 311-323, 2018.

[21] T. Matthews, A. Y. Lo, and J. A. Byrne, "Reconceptualizing green infrastructure for climate change adaptation: Barriers to adoption and drivers for uptake by spatial planners," *Landscape and Urban Planning,* vol. 138, pp. 155-163, 2015.

[22] H. Long, X. Wu, W. Wang, and G. Dong, "Analysis of urban-rural land-use change during 1995-2006 and its policy dimensional driving forces in Chongqing, China," *Sensors,* vol. 8, no. 2, pp. 681-699, 2008.

[23] S. Ullah, K. Ahmad, R. U. Sajjad, A. M. Abbasi, A. Nazeer, and A. A. Tahir, "Analysis and simulation of land cover changes and their impacts on land surface temperature in a lower Himalayan region," *Journal of Environmental Management,* vol. 245, pp. 348-357, 2019.

[24] R. Selçuk, R. Nisanci, B. Uzun, A. Yalcin, H. Inan, and T. Yomralioglu, "Monitoring land-use changes by GIS and remote sensing techniques: case study of Trabzon," in *Proceedings of 2nd FIG Regional Conference, Morocco*, 2003, pp. 1-11.

[25] S. Al-Hathloul and M. A. Rahman, "Dynamism of metropolitan areas: The case of metropolitan Dammam, Saudi Arabia," *Gulf Arab. Penins. Stud,* vol. 29, pp. 11-43, 2003.

[26] J. Li and H. Zhao, "Detecting urban land-use and land-cover changes in Mississauga using Landsat TM images," *Journal of Environment Informatics,* vol. 2, no. 1, pp. 38-47, 2003.

[27] D. R. Streutker, "Satellite-measured growth of the urban heat island of Houston, Texas," *Remote Sensing of Environment,* vol. 85, no. 3, pp. 282-289, 2003.

[28] M. A. Hart and D. J. Sailor, "Quantifying the influence of land-use and surface characteristics on spatial variability in the urban heat island," *Theoretical and applied climatology,* vol. 95, no. 3-4, pp. 397-406, 2009.

[29] A. Lilly Rose, Devadas, M.D., "Analysis of Land Surface Temperature and Land Use/Land Cover Types Using Remote Sensing Imagery - A Case In Chennai City, India," presented at the The seventh International Conference on Urban Climate, Yokohama, Japan, 29 June 2009 - 3 July 2009, 2009.
[30] P. Fu and Q. Weng, "Responses of urban heat island in Atlanta to different land-use scenarios," *Theoretical and applied climatology,* vol. 133, no. 1-2, pp. 123-135, 2018.
[31] D. Niyogi, "Land Surface Processes," in *Current Trends in the Representation of Physical Processes in Weather and Climate Models*: Springer, 2019, pp. 349-370.
[32] R. Thapa and Y. Murayama, "Examining spatiotemporal urbanization patterns in Kathmandu Valley, Nepal: Remote sensing and spatial metrics approaches," *Remote Sensing,* vol. 1, no. 3, pp. 534-556, 2009.
[33] D. Trolle *et al.*, "Effects of changes in land use and climate on aquatic ecosystems: Coupling of models and decomposition of uncertainties," *Science of the Total Environment,* vol. 657, pp. 627-633, 2019.
[34] B. Ahmed, "Urban land cover change detection analysis and modeling spatio-temporal Growth dynamics using Remote Sensing and GIS Techniques: A case study of Dhaka, Bangladesh," 2011.
[35] A. Dewan and R. Corner, *Dhaka megacity: Geospatial perspectives on urbanisation, environment and health*. Springer Science & Business Media, 2013.
[36] I. D. Maduako, Z. Yun, and B. Patrick, "Simulation and prediction of land surface temperature (LST) dynamics within Ikom City in Nigeria using artificial neural network (ANN)," *Journal of Remote Sensing & GIS,* vol. 5, no. 1, pp. 1-7, 2016.
[37] S. Pal and S. Ziaul, "Detection of land use and land cover change and land surface temperature in English Bazar urban centre," *The Egyptian Journal of Remote Sensing and Space Science,* vol. 20, no. 1, pp. 125-145, 2017.
[38] N. Shatnawi and H. Abu Qdais, "Mapping urban land surface temperature using remote sensing techniques and artificial neural network modelling," *International Journal of Remote Sensing,* pp. 1-16, 2019.
[39] D. X. Tran, F. Pla, P. Latorre-Carmona, S. W. Myint, M. Caetano, and H. V. Kieu, "Characterizing the relationship between land use land cover change and land surface temperature," *ISPRS Journal of Photogrammetry and Remote Sensing,* vol. 124, pp. 119-132, 2017.
[40] A. A. Kafy *et al.*, "Impact of LULC Changes on LST in Rajshahi District of Bangladesh: A Remote Sensing Approach," *Journal of Geographical Studies,* vol. 3, pp. 11-23, 01/07 2020.
[41] B. Ahmed, "Modelling spatio-temporal urban land cover growth dynamics using remote sensing and GIS techniques: A case study of Khulna City," *Journal of Bangladesh Institute of Planners,* vol. 4, no. 1633, p. 43, 2011.
[42] B. Ahmed, M. Kamruzzaman, X. Zhu, M. Rahman, and K. Choi, "Simulating land cover changes and their impacts on land surface temperature in Dhaka, Bangladesh," *Remote Sensing,* vol. 5, no. 11, pp. 5969-5998, 2013.
[43] M. Hussain, P. Alak, and I. Azmz, "Spatio-temporal analysis of land use and land cover changes in Chittagong city corporation, Bangladesh," *International Journal of Advancement in Remote Sensing, GIS and Geography,* vol. 4, no. 2, pp. 56-72, 2016.
[44] P. Alo, "Mymensingh now a division," in *Prothom Alo*, ed: Prothom Alo, 2017.
[45] C. Coll, J. M. Galve, J. M. Sanchez, and V. Caselles, "Validation of Landsat-7/ETM+ thermal-band calibration and atmospheric correction with ground-based measurements," *IEEE Transactions on Geoscience Remote Sensing,* vol. 48, no. 1, pp. 547-555, 2009.
[46] K. S. Kumar, P. U. Bhaskar, and K. Padmakumari, "Estimation of land surface temperature to study urban heat island effect using LANDSAT ETM+ image," *International journal of Engineering Science and technology,* vol. 4, no. 2, pp. 771-778, 2012.
[47] A. Rasul, H. Balzter, and C. Smith, "Spatial variation of the daytime Surface Urban Cool Island during the dry season in Erbil, Iraqi Kurdistan, from Landsat 8," *Urban Climate,* vol. 14, pp. 176-186, 2015.
[48] M. Scarano and J. Sobrino, "On the relationship between the sky view factor and the land surface temperature derived by Landsat-8 images in Bari, Italy," *International Journal of Remote Sensing,* vol. 36, no. 19-20, pp. 4820-4835, 2015.
[49] G. Gutman, C. Huang, G. Chander, P. Noojipady, and J. G. Masek, "Assessment of the NASA–USGS global land survey (GLS) datasets," *Remote Sensing of Environment,* vol. 134, pp. 249-265, 2013.
[50] D. P. Roy *et al.*, "Landsat-8: Science and product vision for terrestrial global change research," *Remote sensing of Environment,* vol. 145, pp. 154-172, 2014.
[51] X. Yu, X. Guo, and Z. Wu, "Land surface temperature retrieval from Landsat 8 TIRS—Comparison between radiative transfer equation-based method, split window algorithm and single channel method," *Remote Sensing,* vol. 6, no. 10, pp. 9829-9852, 2014.
[52] G. T. Yengoh, D. Dent, L. Olsson, A. E. Tengberg, and C. J. Tucker III, *Use of the Normalized Difference Vegetation Index (NDVI) to Assess Land Degradation at Multiple Scales: Current Status, Future Trends, and Practical Considerations*. Springer, 2015.
[53] M. Gascon *et al.*, "Normalized difference vegetation index (NDVI) as a marker of surrounding greenness in epidemiological studies: The case of Barcelona city," *Urban Forestry and Urban Greening,* vol. 19, pp. 88-94, 2016.
[54] U. Avdan and G. Jovanovska, "Algorithm for automated mapping of land surface temperature using LANDSAT 8 satellite data," *Remote Sensing,* vol. 2016, 2016// 2016.
[55] IPCC, "Mitigation of climate change," *Contribution of Working Group III to the Fifth Assessment Report of the Intergovernmental Panel on Climate Change,* vol. 1454, 2014.
[56] W. Bank, "Climate Change & Sustainable Report- Bangladesh," 2016.
[57] M. Alamgir *et al.*, "Evaluating severity–area–frequency (SAF) of seasonal droughts in Bangladesh under climate change scenarios," *Stochastic Environmental Research and Risk Assessment,* pp. 1-18, 2020.
[58] UNB, "Bangladesh set to see shorter, warmer winter again. ," in *The Business Standard*, ed. https://tbsnews.net/environment/bangladesh-set-see-shorter-warmer-winter-again-experts, 2019.
[59] Å. Kolås, L. Barkved, K. Edelen, K. Hoelscher, F. Jahan, and H. B. Jha, "Water Scarcity in Bangladesh," 2000.